

Magnetic chitosan/clay beads: A magsorbent for the removal of cationic dye from water

Agnès Bée, Layaly Obeid, Rakotomalala Mbolantenaina, Mathias Welschbillig, Delphine Talbot

► **To cite this version:**

Agnès Bée, Layaly Obeid, Rakotomalala Mbolantenaina, Mathias Welschbillig, Delphine Talbot. Magnetic chitosan/clay beads: A magsorbent for the removal of cationic dye from water. *Journal of Magnetism and Magnetic Materials*, Elsevier, 2017, 421, pp.59-64. 10.1016/j.jmmm.2016.07.022 . hal-01368498

HAL Id: hal-01368498

<https://hal.sorbonne-universite.fr/hal-01368498>

Submitted on 19 Sep 2016

HAL is a multi-disciplinary open access archive for the deposit and dissemination of scientific research documents, whether they are published or not. The documents may come from teaching and research institutions in France or abroad, or from public or private research centers.

L'archive ouverte pluridisciplinaire **HAL**, est destinée au dépôt et à la diffusion de documents scientifiques de niveau recherche, publiés ou non, émanant des établissements d'enseignement et de recherche français ou étrangers, des laboratoires publics ou privés.

Magnetic chitosan/clay beads: a magsorbent for the removal of cationic dye from water

Agnès Bée^{a,*}, Layaly Obeid^{a,b}, Rakotomalala Mbolantenaina^a, Mathias Welschbillig^b,
Delphine Talbot^a

agnes.bee@upmc.fr, lghannoum@hotmail.fr, mbolantenaina@yahoo.fr,
welschbillig@certinergysolutions.com, delphine.talbot@upmc.fr

^a Sorbonne Universités, UPMC Univ Paris 06, CNRS, Laboratoire PHENIX, F-75005 Paris, France

^b CertiNergy Solutions 33 avenue du Maine – BP 195 – 75755 Paris Cedex 15

* Corresponding Author :

Mail: agnes.bee@upmc.fr

Tel: 33 1 44 27 30 98

Address: Sorbonne Universités, UPMC Univ Paris 06, UMR 8234, PHENIX, case 51, 4 place Jussieu, F-75005 Paris, France

Abstract

A magnetic composite material composed of magnetic nanoparticles and clay encapsulated in cross-linked chitosan beads was prepared, characterized and used as a magsorbent for the removal of a cationic dye, methylene blue (MB), from aqueous solutions. The magnetic properties of these beads represent an advantage to recover them at the end of the depollution process. The optimal weight ratio $R=\text{clay:chitosan}$ for the removal of MB in a large range of pH was determined. For beads without clay, the maximal adsorption capacity of MB occurs in the pH range [9-12], while for beads with clay, the pH range extends by increasing the amount of clay to reach [3-12] for $R>0.5$. Adsorption isotherms show that the adsorption capacity of magnetic beads is equal to 82 mg/g. Moreover, the kinetics of dye adsorption is relatively fast since 50% of the dye is removed in the first 13 min for an initial MB concentration equal to 100mg/L. The estimation of the number of adsorption sites at a given pH shows that the main driving force for adsorption of MB in a large range of pH is the electrostatic interaction between the positively charged dye and the permanent negative charges of clay.

Keywords: Ferrofluid, chitosan, magnetic, adsorption, clay, dye

1 Introduction

During the last few decades, the treatment of effluents has become a challenge in the environmental field due to the presence of numerous pollutants in the environment coming from human activity. Indeed, the processes currently used for the removal of pollutants have to be improved to increase their efficiency in terms of abatement of pollution, of decrease of sludge production and, sometimes for recovering materials of economical interest. Among the methods used for the water treatment, adsorption process is currently considered as an efficient and economic method for the removal of pollutants. Its easy handling and its minimal sludge production are important assets to use such a process in the water treatment although its success is strongly dependent of the chosen adsorbent. Adsorption studies with green, efficient and low-cost adsorbents have already shown remarkable results but efforts are still needed to find a way for separating pollutants and adsorbents from the water being treated. In this framework, magnetic composites attract increasing research attention due to both their adsorption efficiency and their magnetic properties. Indeed, magnetic systems can be easily separated and collected by applying an external magnetic field allowing removal of pollutants from water but also recovery of the adsorbent, thereby preventing an increase in the turbidity of the water being treated. Researchers have developed many systems combining a magnetic material with other compounds. We focus therefore our attention on magnetic composites based on biopolymer and clay. Due to their environmental-friendly properties, the combination of clay and biopolymer appears as an attractive way to develop materials with properties that are inherent to the different components. Among natural polymers, chitosan is a good candidate to develop organic-inorganic hybrid materials. Chitosan is the deacetylated product of chitin, a natural polymer found in the cell wall of fungi or in the exoskeletons of crustaceans and insects. Chitosan is a copolymer composed of D-glucosamine and N-acetyl-D-glucosamine units. Its adsorption properties are mainly governed by the acid-base properties of the amine group. In particular, the formation of protonated groups $R-NH_3^+$ contributes to the solubility of chitosan in acid medium. To prevent this dissolution, a crosslinking agent is used, that contributes to maintain chitosan into a bead form, even in acid medium. Indeed, cross-linking produces inter chains linkages using covalent bonding between the polymer chains, which induces the formation of a three dimensional network. The mobility of the chains of the polymer is then reduced and it becomes insoluble in water [1]. Clays are also low-cost adsorbents that are often used as cations exchanger due to their net negative charge [2]. If adsorption of pollutants by magnetic chitosan [3–5] or chitosan-clay composites [6,7] has been widely studied in the literature, there is much less work with

magnetic chitosan-clay composites [8–10]. Moreover, the nature of adsorption sites and the adsorption mechanisms have not gained enough attention.

In the present study, the use of chitosan (CS) beads containing magnetic nanoparticles and clay appears as an improving way to develop materials efficient for adsorption of both anionic and cationic pollutants. The magnetic nanoparticles aid to separate the adsorbent from wastewater after use. The magnetic material which was used for this study is a ferrofluid consisting of magnetic nanoparticles of maghemite bearing surface charges, whose the nature and the number vary with the pH of the medium. In a previous work, magnetic chitosan beads without clay were used for the removal of methyl orange (MO), an anionic dye [11]. MO adsorption occurs in a pH range [3-7], whereas no MB adsorption occurs in this pH range. The encapsulation of clay within the beads aims to extend the pH range for adsorption of MB. Finally, according to the pH value and the quantity of clay in the beads, the adsorbent can remove MB or MO separately or together. These two dyes have been used as models to understand the behavior of cationic and anionic pollutants due to the easiness to determine their concentration in water by UV-Vis spectrophotometry. But they also represent a significant source of water pollution since they are present in the effluents of many industries such as textile, food processing, cosmetics... Magnetic composites were characterized by TGA, atomic absorption spectrometry and X-ray diffraction. Moreover, for a better understanding of the adsorption mechanisms, an estimation of the amounts of adsorption sites has been done. Batch experiments were then carried out to investigate the effects of pH value, contact time, amount of encapsulated clay and initial dye concentration on the adsorption of the dyes by the magnetic beads.

2 Materials and methods

2.1 Materials

We used a clay made available by the company “Eau & Industrie”. It is mainly composed of montmorillonite and will be subsequently called MMT. Its cationic exchange capacity (CEC), determined by adsorption of methylene blue, is equal to 0.47 ± 0.03 mmol/g_{MMT} (47 mequiv/100g). CEC represents the amount of negative adsorption sites of MMT (N_{MMT}^-), which remains constant in the whole pH range.

Chitosan (CS) was characterized by its degree of deacetylation (DDA) (ratio of amino units to total units). It was supplied by Sigma with a DDA of 73.1%. The amino content of chitosan, equal to 4.4 ± 0.2 mmol/g_{CS}, was determined as previously by potentiometric titration [11]; the deduced value of DDA is equal to $71 \pm 4\%$ in accordance with the value given by the

supplier. A mean value of 6.2 is presented in the literature for the pKa of amino groups of chitosan [12]. To estimate the amount of positive adsorption sites of chitosan at a given pH (N_{CS}^+), we considered chitosan as a weak acid. By assuming that the amino content of chitosan represents the maximum positive adsorption sites ($N_{CS,max}^+$), N_{CS}^+ was estimated from the following equation: $N_{CS}^+ = N_{CS,max}^+ / 10^{pH-pKa}$.

Magnetic material was a ferrofluid composed of maghemite ($\gamma\text{-Fe}_2\text{O}_3$) nanoparticles synthesized according to the Massart's method [13,14] and dispersed in diluted nitric acid ($pH \approx 2$). This magnetic material is a polydisperse system of rocklike nanoparticles, which can be described as spheres. The magnetization curve of the ferrofluid was obtained at room temperature using a homemade vibrating sample magnetometer. The mean diameter of the magnetic nanoparticles (d_0) and their polydispersity index (σ), deduced from a two-parameter fit of the magnetization curve, are equal to 7.5 nm and 0.4 respectively [15]. The iron concentration of the ferrofluid, obtained by atomic absorption spectrometry, is equal to 1.49 ± 0.03 mol/L ($119.2 \text{ g}_{\text{maghemite}}/\text{L}$). The stability of the ferrofluid comes from surface charges due to the ionization of hydroxyl groups at the surface of the nanoparticles. Surface density of charges of the nanoparticles could be controlled through pH variations. At the point of zero charge (PZC) located at about pH 7.3, the net surface charge of the particles is zero. At this point, the electrostatic repulsions between uncharged particles do not exist any more and ferrofluid flocculates. Under acidic conditions ($pH < \text{PZC}$) protonation of surface hydroxyl groups leads to a positive surface while their deprotonation leads to a negative surface under alkaline conditions ($pH > \text{PZC}$). Potentiometric measurements allow calculating the amount of charges due to the nanoparticles for a given pH, which represents the adsorption sites of the nanoparticles [16]. After synthesis, the pH value of the ferrofluid was close to 2, the hydroxyl groups are protonated and the particles are then cationic ones with nitrate counterions.

Methylene blue (MB) was purchased from Sigma-Aldrich. Stock solutions of MB were obtained by dissolving the powder in distilled water. Their concentrations were measured by using a UV-Visible Hitachi U2000 spectrophotometer at $\lambda = 664 \text{ nm}$. The extinction coefficient ϵ_{664} is equal to $83243 \text{ molL}^{-1} \text{ cm}^{-1}$. Dye solutions of different initial concentrations were then prepared by diluting the stock solution.

2.2 Magnetic beads synthesis and characterization methods

The synthesis protocol of the magnetic chitosan beads with encapsulated clay was adapted from the one used previously to obtain magnetic chitosan beads without clay [11]. Briefly 15 mL of ferrofluid were added under stirring to a solution containing 3 g (m_{CS}) of chitosan

dissolved in acetic acid; the weight ratio m_{CS}/m_{magh} was equal to 1.2 ± 0.1 , m_{magh} , being the weight of maghemite determined from the iron concentration of the ferrofluid. m_{MMT} g of clay were then added in the mixture to obtain a weight ratio $R = m_{MMT}/m_{CS}$ varying from 0 to 1.3. The mixture was then dropped into NaOH. After that an alkaline epichlorohydrin solution was used as a cross-linking agent to form the chitosan gel. No release of both magnetic nanoparticles and clay was observed in the NaOH bath and during the cross-linking step. The beads were gathered with a magnet and washed with ethanol and deionized water until the $AgNO_3$ test proved the absence of residual chloride ions in the solution. The ready-for-use beads were stored in deionized water and carefully characterized before studying their adsorption properties. Their mean diameter and size distribution were obtained from digitized photographs in combination with image analysis software (ImageJ). The iron content of the beads was analyzed by atomic absorption spectrometry using a Perkin-Elmer AAnalyst100 apparatus. X-ray diffraction studies of air-dried beads ($70^\circ C$) ground to powder were performed on a Rigaku Ultima IV diffractometer using $Cu K\alpha$ radiation. Thermogravimetric analysis were carried out with a SDT Q600 TA Instruments, the heating rate was $10^\circ C/min$. The moisture content ($\%hum = (m_w - m_d)/m_w$) of the beads was determined from the weights of wet (m_w) and dried (m_d) beads.

2.3 Adsorption experiments

Batch adsorption experiments were carried out at room temperature ($\approx 20^\circ C$). Wet magnetic beads ($m_{beads} \approx 0.5g$) were added to 5mL of MB at an initial concentration C_0 . The pH of the samples was controlled using either HNO_3 or NaOH solution. The beads were removed magnetically at predetermined times and the concentration of MB remaining in solution was measured by spectrophotometry. The amount of adsorbed dye, obtained using a mass balance equation, is expressed in millimoles of MB per unit weight of dry beads (mmol/g). The experiments carried out with methyl orange were performed in the same conditions as for MB.

3 Results and discussion

3.1 Characterization of the magsorbent

The millimetric beads are roughly spherical, they appeared brown due to the ferrofluid encapsulation (Figure 1). Due to their magnetic properties, the beads are efficiently attracted to the magnet put in contact with the outside wall of the bottle and thus easily separated from the solution.



Figure 1: Photo of magnetic beads

The size of the wet beads was obtained by using shape-recognition software. The distribution of diameters was fitted by a Gaussian distribution; the obtained mean diameters and standard deviations are reported in Table 1. Even if we may eventually notice a slight decrease of the diameter for beads containing larger amounts of clay, no significant variation occurs with R and a diameter equal to 3.4 mm will be retained.

R	D (mm)	%hum
0 *	-	97.6±0.2
0	3.4±0.2	94.6±0.7
0.1	3.4±0.1	93.3±0.5
0.25	3.4±0.2	92.8±0.1
0.35	-	93.6±0.1
0.5	3.4±0.1	94.5±0.4
0.65	-	92.7±0.1
0.75	3.5±0.1	93.2±0.1
1	3.6±0.2	91.5±0.8
1.1	2.8±0.1	89.2±0.5
1.3	-	91.2±0.5

Table 1: Characterization of the magnetic beads (*beads without clay and magnetic nanoparticles)

Overall, the moisture content of the beads decreases as R increases (Table 1). It is equal to 97.6% for chitosan beads (without nanoparticles and without clay), 94.6% for magnetic chitosan beads without clay (R=0) to stabilize at approximately 91.5% for $R \geq 1$. This decrease is due to the increase of the mineral fillers by increasing the clay content in the beads. A strengthening of the beads then occurs, which reduces their swelling. As expected, the maghemite content within the beads (w_{magh}) also decreases when R increases. Figure 2 shows that the values of w_{magh} obtained from the determination by atomic adsorption spectrometry of iron concentration in the beads ($w_{\text{magh,AAS}}$) are in agreement with those calculated from the amount of ferrofluid introduced in the initial mixture ($w_{\text{magh,c}}$).

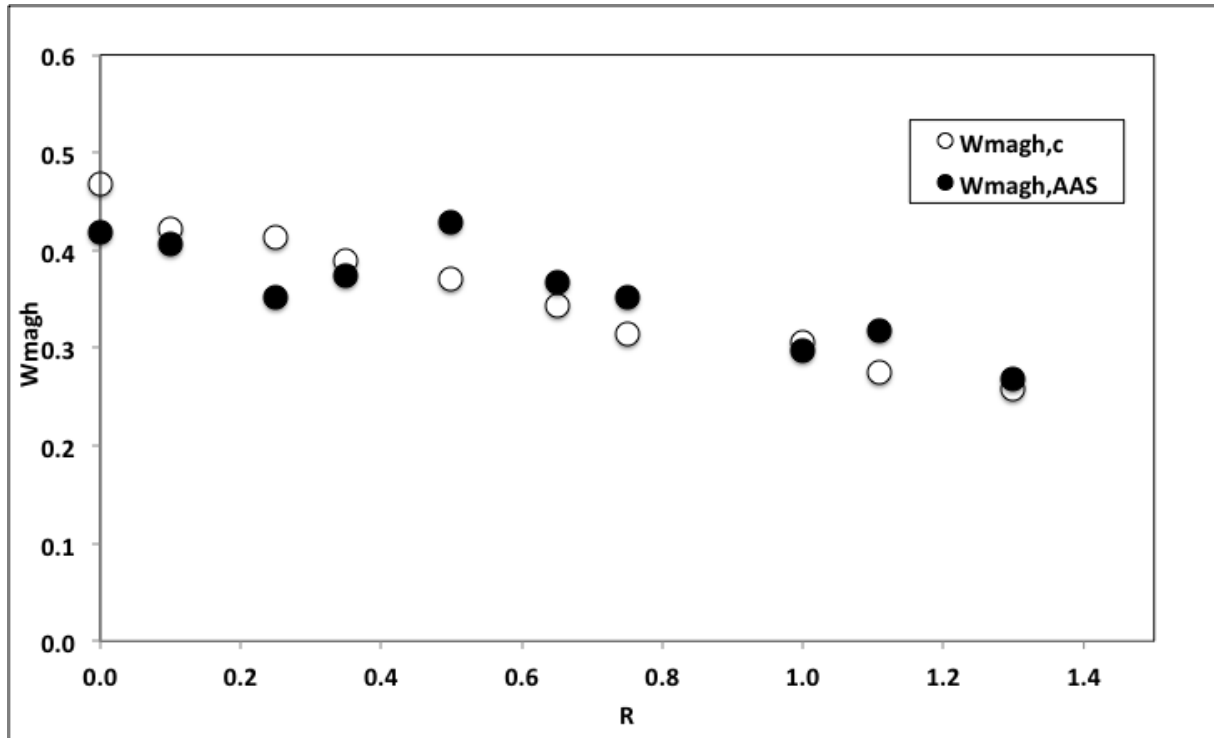


Figure 2: Variation of the maghemite content in the beads with R.

XRD pattern of magnetic beads ($R=0.75$) reported in Figure 3 is compared with those of clay and magnetic nanoparticles. The diffractogram of the magnetic nanoparticles shows diffraction peaks ($2\theta=30.2^\circ$, 35.5° , 43.2° , 53.7° , 57.2° and 62.9°) corresponding to the indices (220), (311), (400), (422), (511) and (440), which are consistent with the referenced data for maghemite (JCPDS 39-1346). Clays are almost always mixed with non-clays minerals, which can produce intense peaks, even when they are in small quantities. As it is shown on Figure 3, the clay used is not pure montmorillonite, the most intense peak at $2\theta=26.7^\circ$ is due to the presence of quartz (JCPDS 5-0490). Magnetic beads diffractogram display diffraction peaks similar to that of both magnetic nanoparticles and clay, which indicates that the two compounds are efficiently encapsulated.

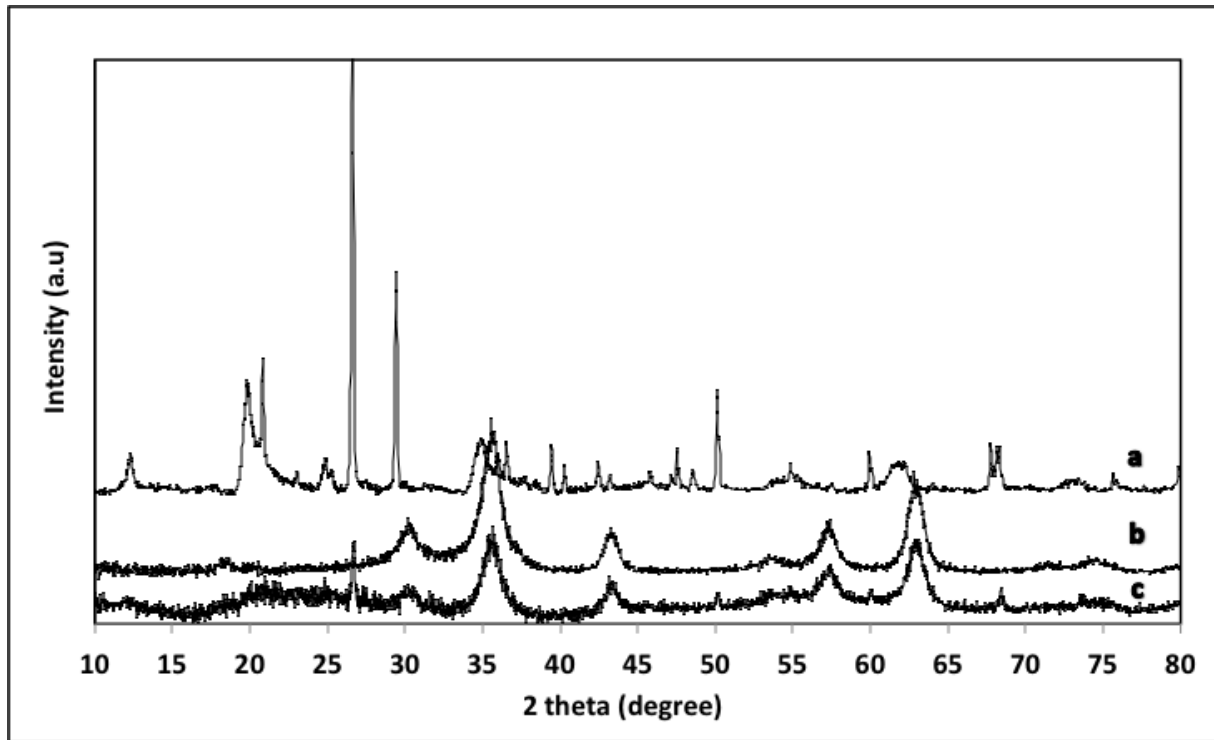


Figure 3: XRD patterns of clay (a), magnetic nanoparticles (b) and magnetic beads (R=0.75) (c).

Figure 4 shows the thermogravimetric analysis (TGA) curves from 20°C to 600°C for magnetic beads (R=0.75) and precursor compounds (chitosan, clay and maghemite nanoparticles). The TGA curve of clay shows a weight loss of 10.0% (below 200°C with a peak at 47°C) and 4.0% (between 300°C and 600°C with a peak at 460°C) attributed to the losses of free water (between particles and on the external surface) and interlayer water respectively [17]. The TGA curve of maghemite nanoparticles shows a weight loss of 4% (up to 150°C) and 6% (between 150°C and 420°C) due to physically and chemically adsorbed water respectively [18]. After a first weight loss of about 10% due to loss of water, the first thermal degradation of chitosan occurs at 240-340°C with a peak at 312°C and a weight loss of 37%. It was attributed to the first stage of pyrolysis, when dehydration, depolymerization and decomposition of acetylated and desacetylated units occur [19]. It is followed by a second degradation of chitosan with a peak at 547°C, the total decomposition occurring for temperatures higher than 600°C [20]. In the case of magnetic beads (R=0.75), after a first weight loss of about 8% due to loss of water, a weight loss of 40%, is also observed, which is mainly due to the decomposition of chitosan. By assuming that the ratios $\left(\frac{m_{CH}}{m_{magh}}\right)$ and $\left(\frac{m_{MMT}}{m_{magh}}\right)$ remain the same in the beads than in the initial mixture (before crosslinking) and knowing the amount of maghemite in the beads from the determination of iron, the mass fractions of the different components in the beads can then be calculated. Considering that the

weight loss in the beads is the sum of the weight losses of their different components, the expected weight loss for the beads can be estimated from the mass fractions. It is found to be equal to 43%, this value being close to the experimental value.

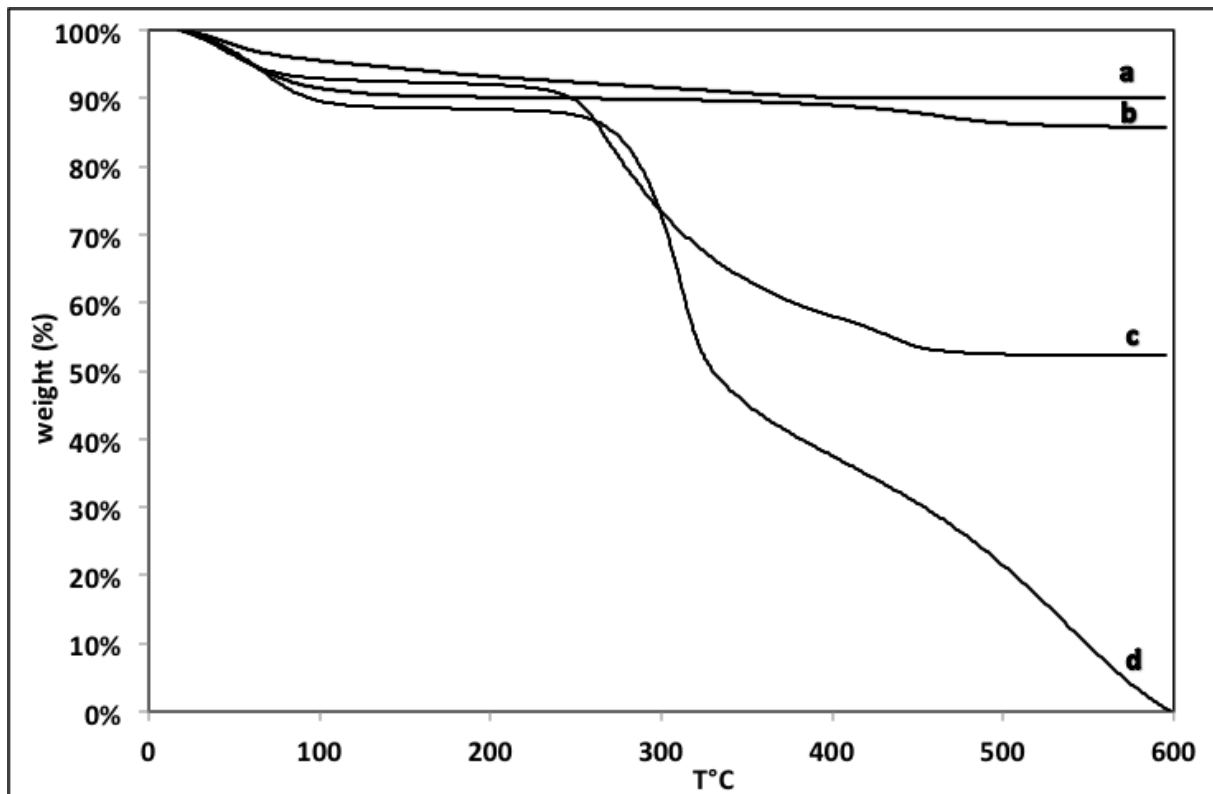


Figure 4: TGA curves for magnetic nanoparticles (a), clay (b), magnetic beads (R=0.75) (c) and chitosan (d); heating rate of 10°C/min.

Additionally, the quantity of adsorption sites of the magnetic beads was estimated from the quantity of sites coming from chitosan, magnetic nanoparticles and clay assuming that there is no interaction between the different constituents of the beads. Chitosan bears positive charges in acidic medium due to its amine functions, magnetic nanoparticles bear positive charges at pH below pH_{PZC} and negative charges at pH higher than pH_{PZC} , while clay bears permanent negative charges regardless of the pH of the solution. For the synthesis of the beads, we used positively charged magnetic nanoparticles to avoid the possibility of self-assembly between nanoparticles and positively charged chitosan before the crosslinking step. This method keeps the sites of particles available for adsorption of dye molecules. Figure 5 shows an example of the evolution of adsorption sites as a function of pH for magnetic beads (R=0 and 1.3). It has to be noted that before pH_{PZC} of the nanoparticles, the negative charges of the beads (N^-) come only from clay.

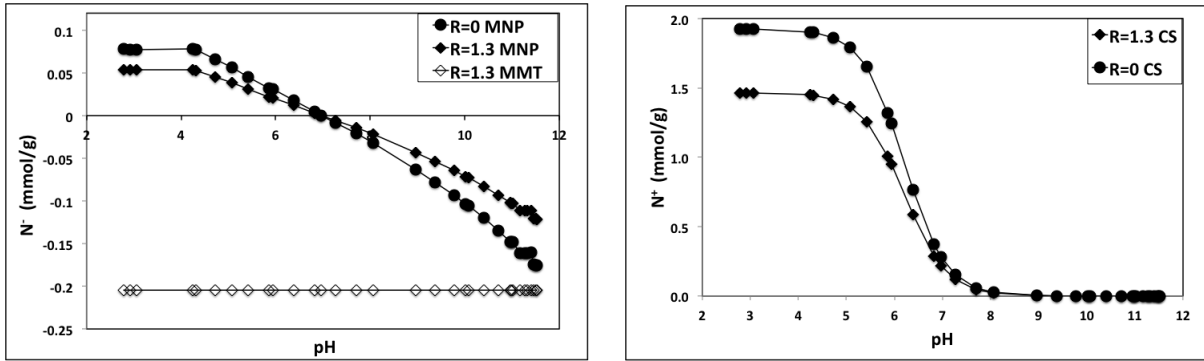


Figure 5: Evolution of adsorption sites (N) of magnetic beads ($R=0$ and 1.3) as a function of pH. Left: negative sites due to magnetic nanoparticles (MNP) and clay (MMT), right: positive sites due to chitosan (CS).

3.2 Adsorption properties of the beads

3.2.1 Effect of contact time on adsorption

The variation in percentage removal of MB with contact time at an initial concentration of 100 mg/L is shown on Figure 6 for $R=0.1$, 0.75 and 1 at an initial pH close to 6.5 . In all the cases, 50% of MB is quickly removed in the first 13 min (Table 2). Then adsorption becomes slower probably due to the reduced availability of clay sites in the beads. The time to reach 90% adsorption is equal to 1.7h for $R=0.1$ and slightly increases with R .

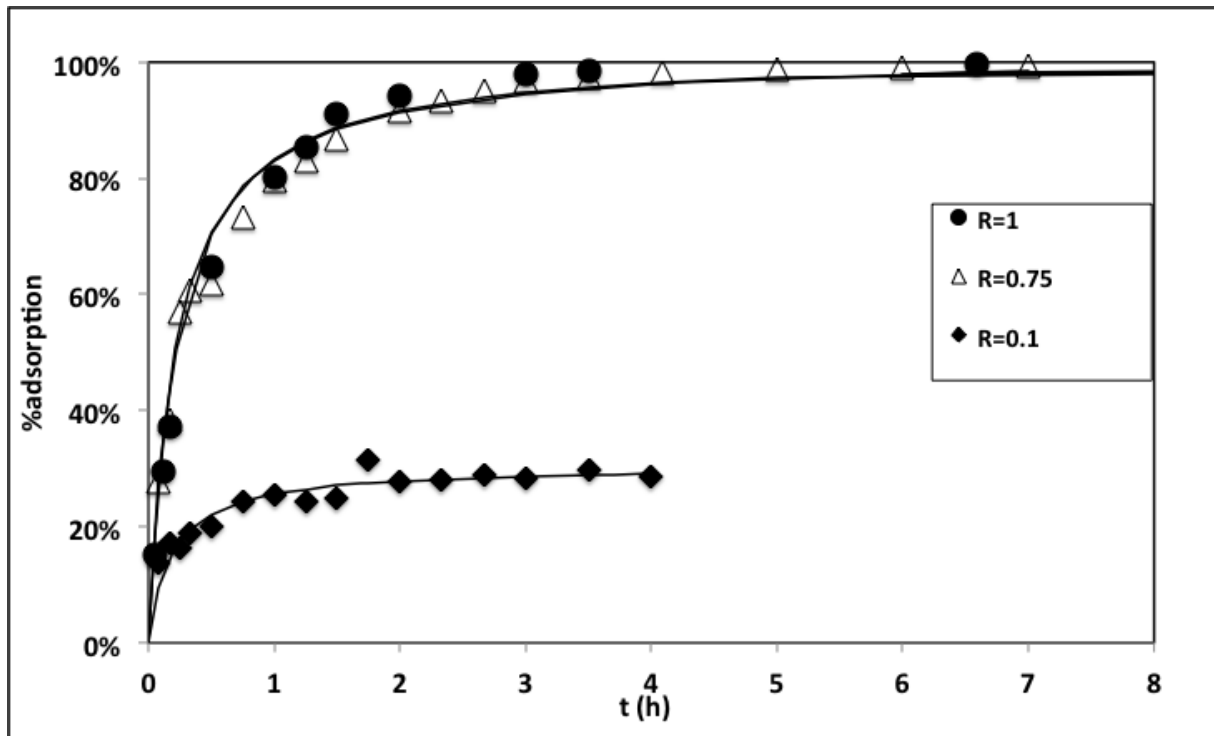


Figure 6: Effect of contact time on the extent of MB adsorption.

At equilibrium, MB removal is only 28.5% for R=0.1, whereas 99% adsorption is observed for R=0.75 and R=1. As the pH of the study is close to the point of zero charge of the magnetic nanoparticles, their contribution to MB adsorption is not significant. The negative charges of clay (noted N_{MMT}^-), which increase with R, are then mainly responsible of MB adsorption (Table 2). For R=0.1, the amount of negative adsorption sites is not sufficient to adsorb all the added dye molecules. While for R=0.75 and 1, the amount of available negative sites is significantly higher than the quantity of dye and so widely sufficient to obtain almost 100% adsorption even if it remains positive charges from chitosan (noted N_{CS}^+).

R		0.1	0.75	1
C_0	mmol/g	0.042	0.039	0.031
Q_{eq}	mmol/g	0.012	0.038	0.030
	%	28.5	99.2	98.7
t_{50}	min	11	13	13
t_{90}	h	1.7	1.9	2.0
N_{MMT}^-	mmol/g	-0.020	-0.149	-0.169
N_{CS}^+	mmol/g	0.264	0.284	0.218

Table 2: Kinetics parameters (Q_{eq} : amount of dye adsorbed at equilibrium; t_x : time to reach x% of the adsorbed dye at equilibrium).

3.2.2 Effect of pH on adsorption

Magnetic chitosan beads with different weight ratios R were synthesized; the resulting beads were used to find the optimal amount of clay for the most efficient adsorption of MB in the largest pH range.

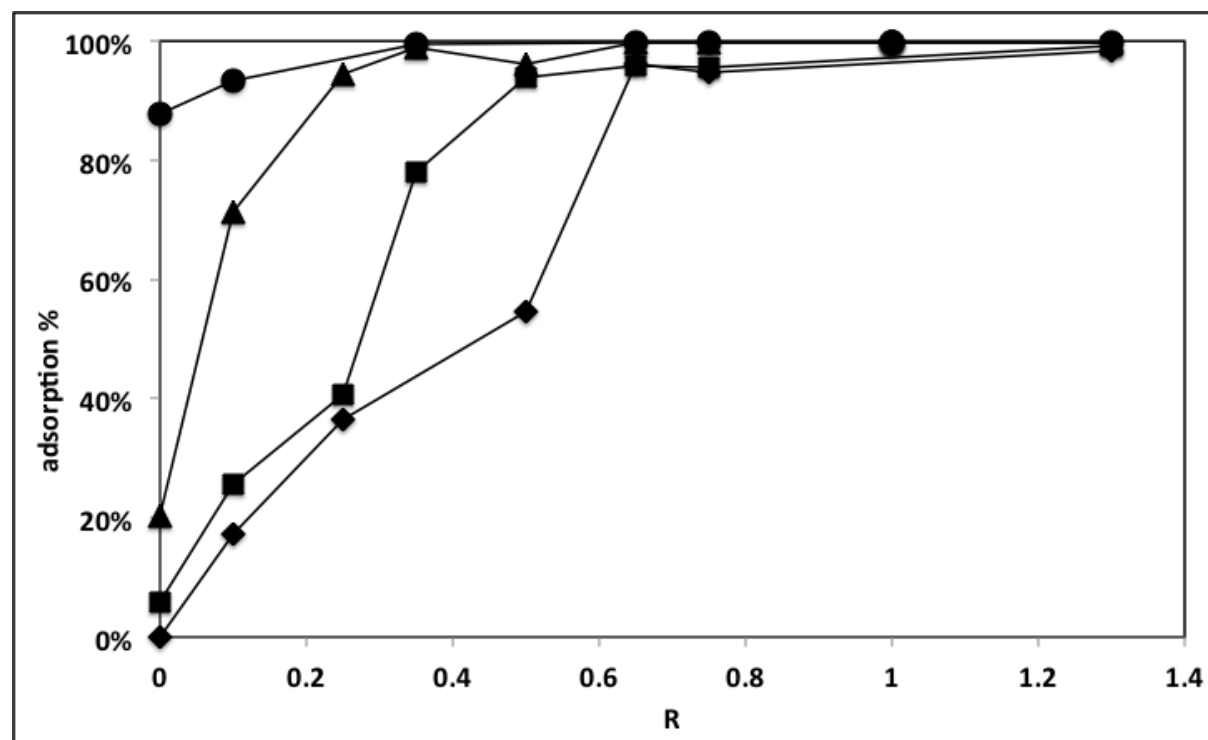


Figure 7 shows the effect of R on MB adsorption ($C_0 = 100\text{mg/L}$) for four pH values. Regardless pH values, MB adsorption increases with R. This increase is particularly pronounced in acid medium where MB is weakly adsorbed by beads without clay or containing little clay. In this case, the positive charge of the beads due to both chitosan and magnetic nanoparticles induces electrostatic repulsions with the positively charged dye. In alkaline medium, the effect of R is less marked. For $R > 0.6$, almost complete removal of the dye is observed for all the pH values.

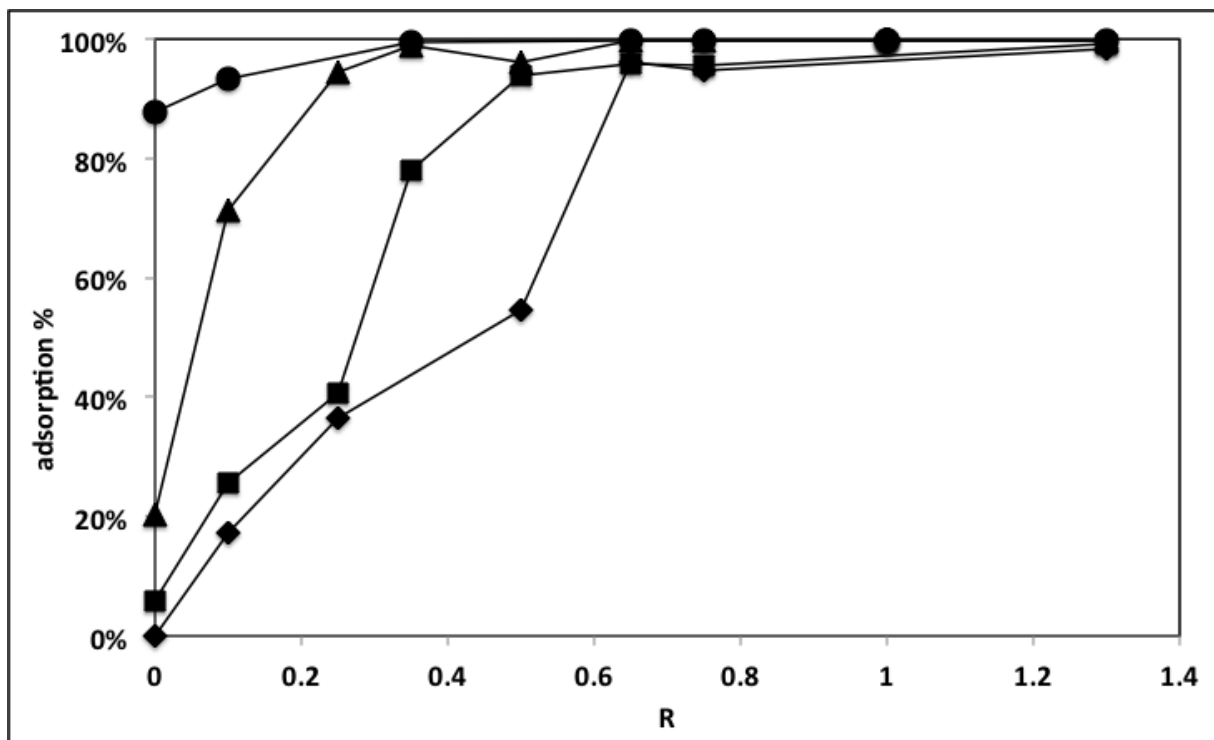


Figure 7: Effect of R on methylene blue uptake for different pH and R values ($C_0=100\text{mg/L}$);

pH: ◆: 3.7 ± 0.4 , ■: 4.7 ± 0.2 , ▲: 7.2 ± 0.2 , ●: 9.4 ± 0.2 .

To understand the adsorption mechanisms, Figure 8 reports the effect of pH on adsorption of MB and MO by magnetic beads without clay. The data for methyl orange (MO), an anionic dye, come from a previous work [11]. For MO, the maximum removal is observed in the pH range 3–5. The nanoparticles and amino groups of chitosan being in their protonated cationic form, the adsorption process is mainly controlled by an ionic exchange mechanism due to coulombic interaction between the positively charged beads and negative functional groups of MO. Above pH 5, adsorption decreases to become almost constant above pH 8. Deprotonation of both amino groups of chitosan and hydroxyl groups of magnetic nanoparticles occur, leading to a decrease of interactions between beads and anionic dye. In alkaline medium, a small amount of dye is still adsorbed (about 15%) owing to Van der

Waals attraction, MO being a polar molecule. In the case of the cationic MB, adsorption presents a maximum at a pH value above 8.5 due to the negative sites of magnetic nanoparticles. A decrease of pH value makes MB adsorption less important due to both the decrease of negative charges of the magnetic nanoparticles and the progressive protonation of chitosan. Below pH about 7, positive charges of both nanoparticles and chitosan induce electrostatic repulsions with MB and the adsorption falls.

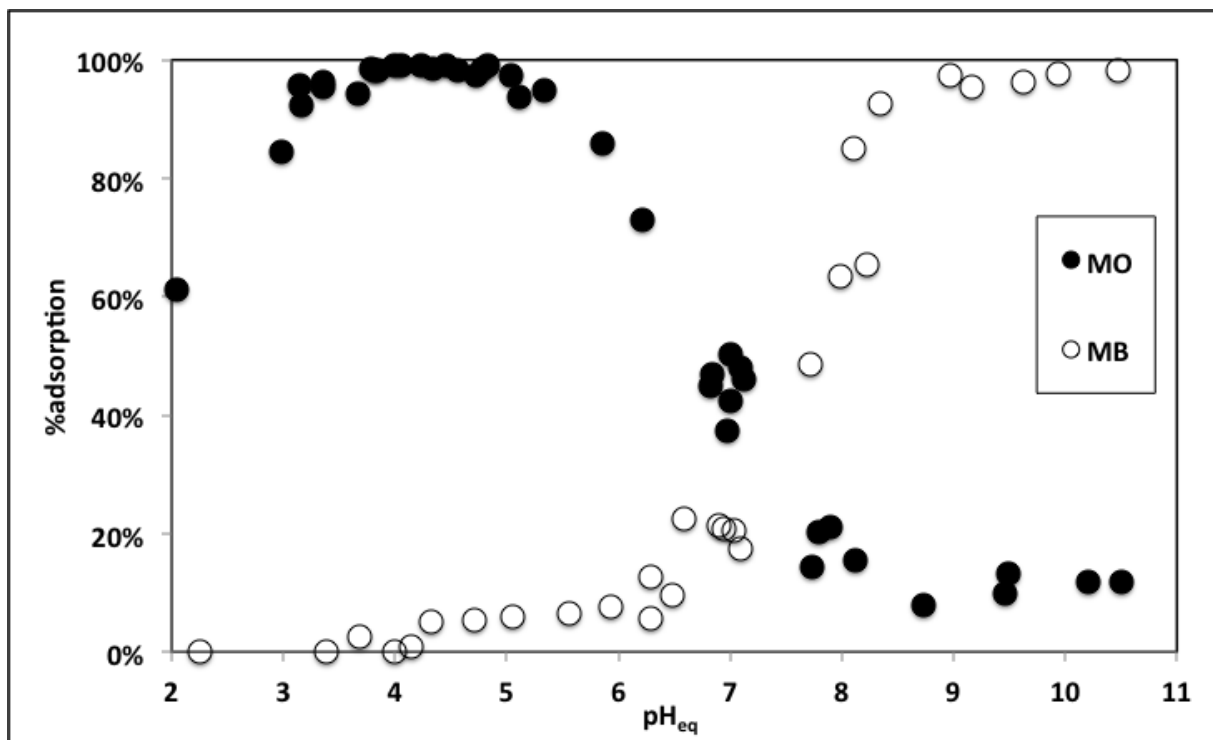


Figure 8: Effect of pH on dye uptake for magnetic beads without clay ($R=0$) ($C_0=100\text{mg/L}$).

In presence of clay, which provides permanent negative charges, the pH range corresponding to the maximum removal efficiency of MB increases with R as it is shown on Figure 9. For $R \geq 0.65$, the adsorption is higher than 92% in the pH range 3-11. Using beads with $R=0.5$, we also checked that clay has no effect on the pH range corresponding to the maximum MO adsorption (not shown). So, in presence of clay, the magnetic beads keep their adsorption properties for anionic compounds and become efficient for adsorption of cationic ones in a large range of pH. The main driving force for adsorption of dyes is the electrostatic interactions i) between the positively charged MB and negatively charged clay and magnetic nanoparticles (for $\text{pH} > \text{pH}_{\text{PZC}}$), ii) between the negatively charged MO and the positively charged chitosan and magnetic nanoparticles ($\text{pH} < \text{pH}_{\text{PZC}}$). The extent of MB adsorption with R is correlated to the increase of permanent negative charges coming from clay, which dominates the positive charges of chitosan.

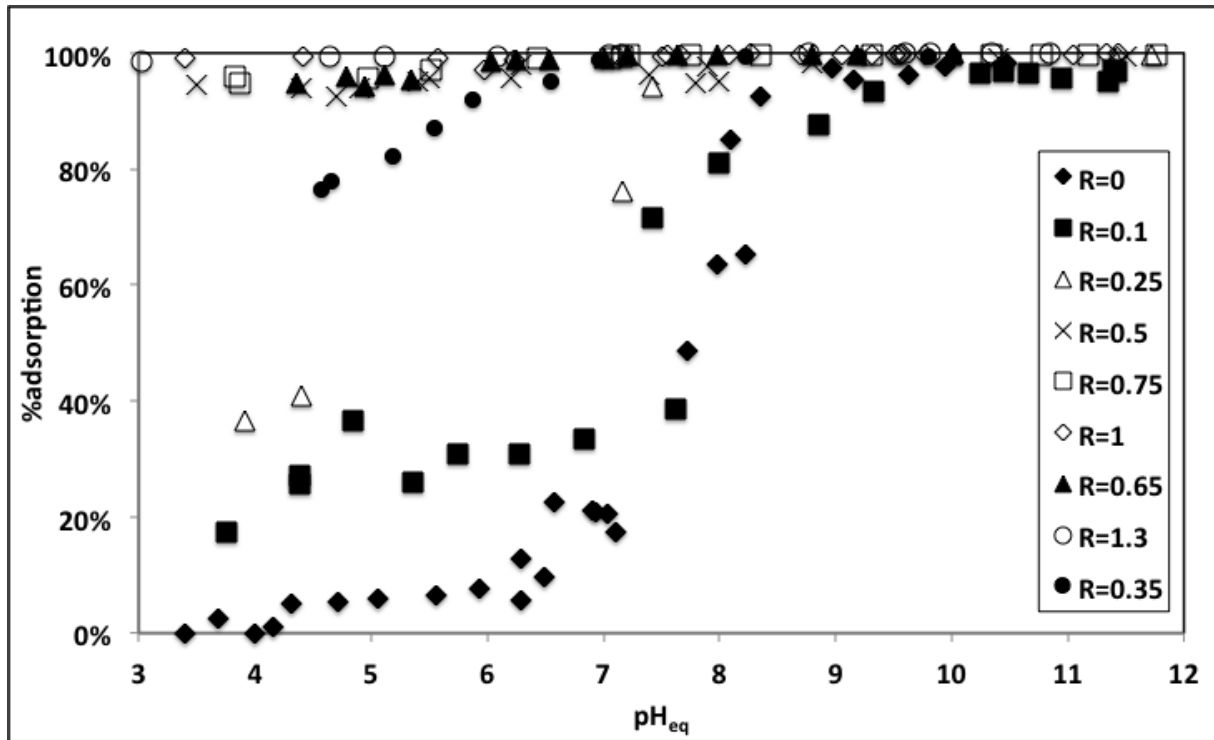


Figure 9: Effect of pH on MB uptake for different R values ($C_0=100\text{mg/L}$).

3.2.3 Adsorption isotherms

The adsorption isotherms, obtained for different R and pH values, represent the evolution of the amount of adsorbed MB (Q_{eq}) with the amount of dye remaining in solution at equilibrium (C_{eq}) (Figure 10). Experiments have been conducted in alkaline medium so that chitosan is not charged, which prevents electrostatic repulsions with the positively charged dye molecules. For the same pH value (about 9.9), the maximum adsorption capacity of the beads increases with R, it is equal to 52 mg/g and 82 mg/g for R=0 and R=1.3 respectively (Table 3). At a value of pH close to pH_{PZC} of the magnetic nanoparticles ($pH=7.6$) and for R=0.75, the adsorption is only due to the presence of clay. On the other hand, at $pH=8.9$ and for R=0.5, even if the amount of clay is weaker, the adsorption does not decrease due to the negative charge of the nanoparticles at this pH.

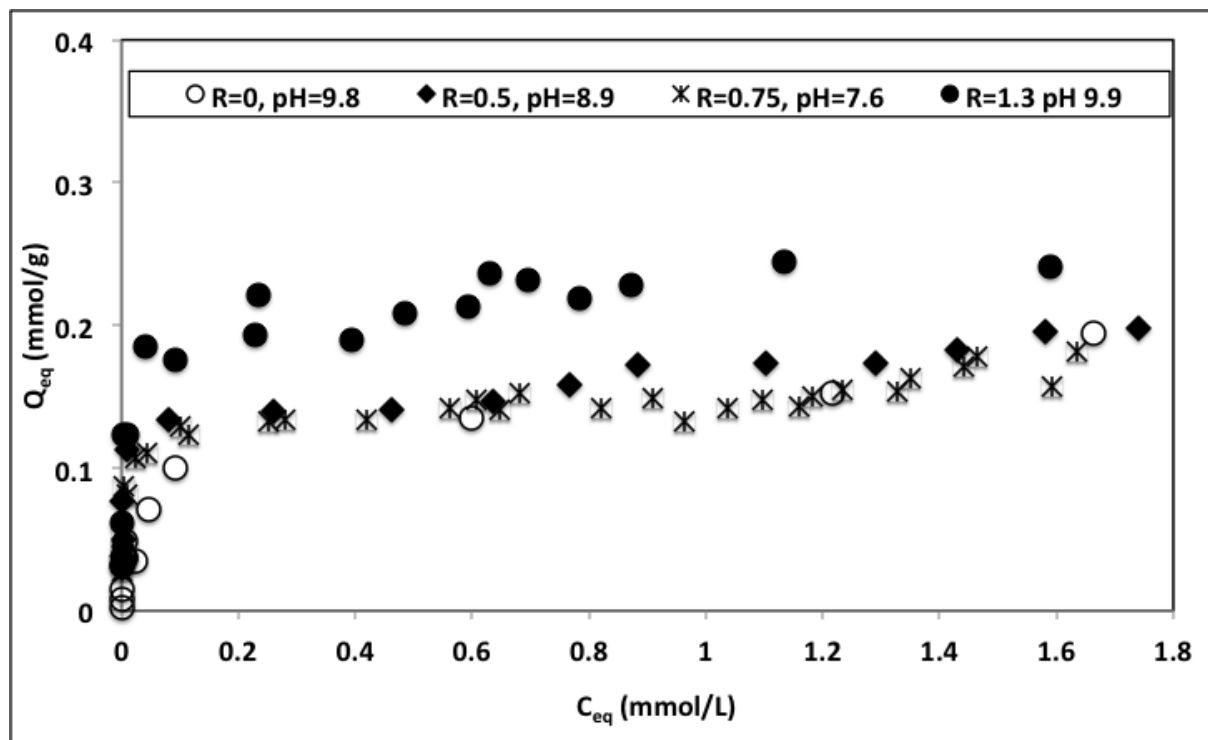


Figure 10: Adsorption isotherms of MB for different R and pH.

Maximum adsorption capacities were also reported to the amount of clay in the beads, the results of the Table 3 show that the values are similar to that obtained from the adsorption isotherm of MB by clay for pH close to pH_{PZC} or higher when the nanoparticles are also involved in the adsorption process. That indicates that adsorption properties of clay are not affected by their encapsulation in the beads. On the other hand, the maximum adsorption capacities are not so far from the estimated negative charges coming from both clay and magnetic nanoparticles calculated at the pH of the isotherms (N^-) (Table 3).

R	pH	$[MB]_{ads,max}$ mmol/g	$[MB]_{ads,max}$ mg/g	$[MB]_{ads,max}$ mmol/gMMT	N^- mmol/g
MMT	≈ 7	-	-	0.47	
R=0	9.8 ± 0.4	0.14	52	-	-0.10
R=0.5	8.9 ± 0.2	0.17	63	0.56	-0.19
R=0.75	7.6 ± 0.3	0.15	56	0.45	-0.17
R=1.3	9.9 ± 0.4	0.22	82	0.51	-0.27

Table 3. Adsorption parameters for MB

4 Conclusion

Herein, we report a simple extrusion method to synthesize a magnetic adsorbent efficient for the removal of MB and, more broadly, of positively charged pollutants. Magnetic composites were prepared by entrapping maghemite nanoparticles and clay in cross-linked chitosan beads. The pH range of the maximum adsorption is strongly correlated to the amount of clay within the beads. For an initial concentration of MB equal to 100mg/L, the removal efficiency

of beads remained at a high level throughout the pH range 3-12 for $R > 0.5$. A maximum uptake of 82 mg/g is obtained for MB at $R = 1.3$ and $\text{pH} = 9.9$. Moreover, it was shown that, independently of R , 50% of dye was quickly removed in the first 13 min of the reaction. Comparison with previously obtained results with a cationic dye, methyl orange, shows that the amount of clay encapsulated in the beads allows monitoring the selectivity of adsorption. Without clay, adsorption of the two dyes occurs in different pH ranges for MB ($\text{pH} > 8.5$) and MO ($3 < \text{pH} < 5$) while for $R \geq 0.5$, an efficient adsorption of the two dyes could be obtained in a same pH range. As a conclusion, according the pH, the magnetic beads developed in this work could be used in wastewater treatment as a multi-functional adsorbent for the removal of both cationic and anionic pollutants separately or together. This is particularly advantageous because wastewaters often contain many contaminants with different behaviors. On the other hand, the beads loaded in pollutants can be easily separated after the completion of the adsorption process in contaminated water by using their magnetic properties without affecting the turbidity of water being treated.

References

- [1] A. Shweta, P. Sonia, Pharmaceutical relevance of cross-linked chitosan in microparticulate drug delivery, *Int. Res. J. Pharm.* 4 (2013) 45–51.
- [2] W. Yan, J. Zhang, C. Jing, Adsorption of Enrofloxacin on montmorillonite: Two-dimensional correlation ATR/FTIR spectroscopy study, *J. Colloid Interface Sci.* 390 (2013) 196–203. doi:10.1016/j.jcis.2012.09.039.
- [3] A. Esmaili, N.T. Farrahi, The efficiency of a novel bioreactor employing bacteria and chitosan-coated magnetic nanoparticles, *J. Taiwan Inst. Chem. Eng.* (n.d.). doi:10.1016/j.jtice.2015.08.022.
- [4] L. Li, H. Duan, X. Wang, C. Luo, Fabrication of novel magnetic nanocomposite with a number of adsorption sites for the removal of dye, *Int. J. Biol. Macromol.* 78 (2015) 17–22. doi:10.1016/j.ijbiomac.2015.01.014.
- [5] V. Sureshkumar, S.C.G. Kiruba Daniel, K. Ruckmani, M. Sivakumar, Fabrication of chitosan–magnetite nanocomposite strip for chromium removal, *Appl. Nanosci.* (2015) 1–9. doi:10.1007/s13204-015-0429-3.
- [6] P. Monvisade, P. Siriphannon, Chitosan intercalated montmorillonite: Preparation, characterization and cationic dye adsorption, *Appl. Clay Sci.* 42 (2009) 427–431. doi:10.1016/j.clay.2008.04.013.
- [7] M. Darder, M. Colilla, E. Ruiz-Hitzky, Biopolymer–Clay Nanocomposites Based on Chitosan Intercalated in Montmorillonite, *Chem. Mater.* 15 (2003) 3774–3780. doi:10.1021/cm0343047.
- [8] D.-W. Cho, B.-H. Jeon, C.-M. Chon, F.W. Schwartz, Y. Jeong, H. Song, Magnetic chitosan composite for adsorption of cationic and anionic dyes in aqueous solution, *J. Ind. Eng. Chem.* 28 (2015) 60–66. doi:10.1016/j.jiec.2015.01.023.
- [9] S. Yang, N. Okada, M. Nagatsu, The highly effective removal of Cs⁺ by low turbidity chitosan-grafted magnetic bentonite, *J. Hazard. Mater.* 301 (2016) 8–16. doi:10.1016/j.jhazmat.2015.08.033.
- [10] W. Zhao, X. Huang, Y. Wang, S. Sun, C. Zhao, A recyclable and regenerable magnetic chitosan absorbent for dye uptake, *Carbohydr. Polym.* 150 (2016) 201–208. doi:10.1016/j.carbpol.2016.05.037.
- [11] L. Obeid, A. Bée, D. Talbot, S.B. Jaafar, V. Dupuis, S. Abramson, V. Cabuil, M. Welschbillig, Chitosan/maghemite composite: A magisorbent for the adsorption of methyl orange, *J. Colloid Interface Sci.* 410 (2013) 52–58. doi:10.1016/j.jcis.2013.07.057.

- [12] Joon Woo Park, Kyung-Hee Choi, Kwanghee Koh Park, Acid-Base Equilibria and Related Properties of Chitosan, *Bull. Korean Chem. Soc.* 4 (1983) 68–72.
- [13] R. Massart, Preparation of aqueous magnetic liquids in alkaline and acidic media, *IEEE Trans. Magn.* 17 (1981) 1247–1248. doi:10.1109/TMAG.
- [14] N. Fauconnier, A. Bee, J. Roger, J.N. Pons, Synthesis of aqueous magnetic liquids by surface complexation of maghemite nanoparticles, *J. Mol. Liq.* 83 (1999) 233–242. doi:10.1016/S0167-7322(99)00088-4.
- [15] J.C. Bacri, R. Perzynski, D. Salin, V. Cabuil, R. Massart, Magnetic Colloidal Properties of Ionic Ferrofluids, *J. Magn. Magn. Mater.* 62 (1986) 36–46. doi:10.1016/0304-8853(86)90731-6.
- [16] A. Ponton, A. Bee, D. Talbot, R. Perzynski, Regeneration of thixotropic magnetic gels studied by mechanical spectroscopy: the effect of the pH, *J Phys Condens Matter.* 17 (2005) 1–16. doi:10.1088/0953-8984/17/6/004.
- [17] W. Xie, Z. Gao, K. Liu, W.-P. Pan, R. Vaia, D. Hunter, A. Singh, Thermal characterization of organically modified montmorillonite, *Mater. Characterization Therm. Anal. Methods.* 367–368 (2001) 339–350. doi:10.1016/S0040-6031(00)00690-0.
- [18] E. Darezereshki, One-step synthesis of hematite (α -Fe₂O₃) nano-particles by direct thermal-decomposition of maghemite, *Mater. Lett.* 65 (2011) 642–645. doi:10.1016/j.matlet.2010.11.030.
- [19] C. Peniche-Covas, W. Argüelles-Monal, J. San Román, A kinetic study of the thermal degradation of chitosan and a mercaptan derivative of chitosan, *Polym. Degrad. Stab.* 39 (1993) 21–28. doi:10.1016/0141-3910(93)90120-8.
- [20] J.H. Kim, J.Y. Kim, Y.M. Lee, K.Y. Kim, Properties and swelling characteristics of cross-linked poly(vinyl alcohol)/chitosan blend membrane, *J. Appl. Polym. Sci.* 45 (1992) 1711–1717. doi:10.1002/app.1992.070451004.